



Cross-layerly embedded FBG in carbon fiber composites for self-modulated, intensity referenced and temperature insensitive microdisplacement measurement



Bo Dong*, Long Xiao, Yandong Gong, Yixin Wang

RF, Antenna & Optical Department, Institute for Infocomm Research, A*STAR, Singapore 138632, Singapore

ARTICLE INFO

Article history:

Received 1 April 2013

Received in revised form 31 May 2013

Accepted 31 May 2013

Available online 14 June 2013

Keywords:

Embedded FBG

Carbon fiber composites

Microdisplacement

ABSTRACT

A novel temperature insensitive and intensity modulated microdisplacement sensor is demonstrated by cross-layerly embedding an FBG in carbon fiber composites. The reflection spectrum of the FBG is self-modulated to be chirped spectrum if a microdisplacement is applied to the center of the sensor structure. By monitoring the optical power change due to the above chirped spectrum variation, the microdisplacement can be measured. Experimental results show that there are quasilinear relationships between the microdisplacement and optical power, the maximum measurement resolution of the sensor reaches 10.7 μm within the displacement range of 0–1050 μm , and the dynamic measurement range is within the range of 0–200 Hz.

© 2013 Elsevier B.V. All rights reserved.

1. Introduction

Fiber-optic sensors have been used to measure lots of physical parameters due to the inherent advantages of immunity to electromagnetic interference and chemical corrosion, light weight, remote sensing ability, and good multiplexing capability. Displacement measurement is one of the primary applications. There are two types of fiber-optic displacement sensors, noncontact and contact ones. Fiber bundle [1–4], fiber-optic Fabry–Perot interferometer [5], and white-light fiber-optic interferometer [6] based noncontact sensors have been developed to meet the requirements for nanometer and even subnanometer displacement measurement. Recently, to meet the requirements for micrometer order displacement measurement, several fiber-optic microdisplacement sensors based on fiber Bragg grating (FBG) [7], long-period fiber grating [8], high-birefringence-fiber loop mirror (HBFLM) [9], photonic crystal fiber interferometer [10] etc., have been proposed. Note that any torsion and outer disturbance applied to the fiber-optic devices will influence the measurement accuracy since they will induce the variations of the measured optical parameters, such as the intensity, wavelength, phase and polarization state etc. Hence, packaging the fiber-optic devices in suitable materials to be practical actuators is important. Although the fiber devices in Refs. [7–9] were surface mounted on the beams, this cannot fully protect the fiber sensor head from outer damage. The fiber-grating- and HBFLM-based

sensors are wavelength modulated, and the wavelength interrogation for the two types of sensors is generally expensive. Moreover, they are also highly sensitive to temperature, which leads to temperature cross sensitivity and limits their practical applications. Hence, using the FBG as low cost, intensity referenced and temperature insensitive sensor is highly desirable, and several methods of using the FBGs as chirped FBG sensors [11–13] have been proposed to realize this. However, they also adopted the methods of surface mounting the FBG on the beams. In addition, for the package material, it should be noted that the carbon-fiber composite is an excellent package material due to its light weight, high toughness, ultrahigh Young's modulus (with tensile modulus of 420 GPa or more), good environmental resistance, etc., and it has been widely used for the aerospace and automotive fields. This type of material is better for the restorability of the packaged sensor.

In this paper, a novel microdisplacement sensor, with a cross-layerly embedded FBG in carbon fiber composites, is demonstrated theoretically and experimentally. As a microdisplacement is applied to the center of the structure, the spectrum of the FBG is self-modulated to be chirped spectrum accordingly. Moreover, this chirp broadens with the increase of the microdisplacement and it is temperature insensitive. By monitoring the reflected optical power variation of the chirped FBG, temperature insensitive microdisplacement measurement is achieved. Experimental results show that there are quasilinear relationships between the displacement and optical power within the measurement ranges of 0–1050, 1200–2100, and 2250–3150 μm , respectively, and the measurement resolutions are 10.7, 29, and 61.3 μm . With the carbon fiber composite as the package material, the sensor shows good

* Corresponding author. Tel.: +65 64082393.

E-mail addresses: bdong@i2r.a-star.edu.sg, dbo1978@163.com (B. Dong).

reproducibility. Moreover, this embedding structure can effectively protect the FBG sensor head from outer disturbance and damage. This type of intensity modulated sensor shows the advantages of temperature insensitiveness, low cost, and good reproducibility.

2. Structure and principle of the sensor

The upper figure in Fig. 1 shows the schematic structure of the sensor. An acrylate-coated FBG, with central wavelength of 1554.618 nm, length of 10 mm, and reflectivity of 95% is cross-layerly embedded in the laminated carbon fiber composites. The thickness of each layer of the composite is 125 μm . The left and right sides of the FBG have 6 layers, respectively, and the transverse distance between the starting points of the two contacted layers is about 2 mm. The FBG is embedded in the central part along the reinforced fiber direction of the two slope composite layers contacted with the FBG, and the reinforced fiber direction of the other layers is parallel. The structure is put in a vacuumized oven for curing at temperature of 120 °C for 120 min. The cured sensor is shown in the below photograph in Fig. 1. Its width, thickness and span are about 8 mm, 1 mm and 7.5 cm, respectively. It can be regarded as a quasi simple supported beam (SSB) with an effective span of L . Based on the theory of material mechanics [14], when a displacement d is vertically applied to the center of the beam within its elastic range, the induced strain ε at any point on the strained layer can be expressed as

$$\varepsilon = \frac{12z}{L^2} d, \quad (1)$$

where z is the distance between the strained and neutral layers. From Eq. (1), it can be seen that linearly varying strain along the thickness is established for the upper and below symmetrical layers, respectively. Under a given displacement, the upper and below symmetrical layers experience the same strain in magnitude but opposite in sign. The crossed layers located with the slanted FBG provide an axial strain gradient along the FBG. The strain transferred to the FBG can be given by

$$\varepsilon = C \frac{12z}{L^2} d \cos \theta, \quad (2)$$

where C is a couple coefficient, describing the strain transfer efficiency from the beam to the FBG; θ is the angle between the axis of the FBG and the central axis of the beam. Assuming the FBG is composed of many small grating segments, the Bragg wavelength change for each small grating is different since each segment experiences different local strain. The relationship between the local axial strain ε applied along the length of the FBG and the Bragg wavelength shift $\Delta\lambda$ can be expressed as

$$\Delta\lambda = \lambda_B (1 - P_e) \varepsilon, \quad (3)$$

where λ_B is the Bragg wavelength of the FBG, and P_e is the effective photoelastic constant of optical fiber. According to Eq. (1), the strain at the neutral lay is zero, and the upper and below symmetrical layers experience the same strain in magnitude but opposite in sign.

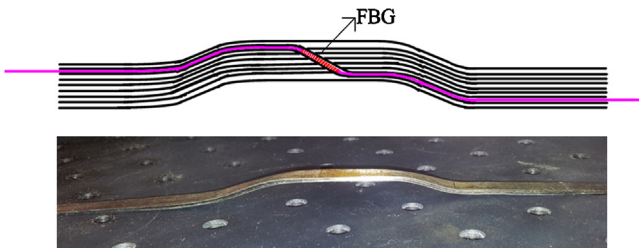


Fig. 1. Schematic structure and the photograph of the sensor.

Hence, for the FBG crossed the neutral layer of the beam, the chirped bandwidth of the FBG is determined by the vertical distances from the upper FBG end to the neutral lay z_u and from the below FBG end to the neutral layer z_b , and their relationship with the length l of the FBG can be expressed as

$$z_u - z_b = l \sin \theta. \quad (4)$$

Hence, the reflection bandwidth of the chirped FBG can be given by,

$$\begin{aligned} \Delta\lambda_{\text{chirp}} &= \lambda_B (1 - P_e) C \frac{12(z_u - z_b)}{L^2} d \cos \theta \\ &= C \lambda_B (1 - P_e) \frac{6l}{L^2} d \sin(2\theta). \end{aligned} \quad (5)$$

If the reflected optical power of the chirped FBG is detected by a photoreceiver or a powermeter, the detected optical power can be expressed as

$$P = \alpha \int T(\lambda) R(\lambda) d\lambda, \quad (6)$$

where α is a coefficient, describing the light path loss efficient from the broadband source to the detector or powermeter, $T(\lambda)$ and $R(\lambda)$ are the power spectral density of the broadband light source and the reflectivity of grating, respectively, and they are functions of wavelength λ . For the broadband source with a flat power spectrum, $T(\lambda)$ is a constant. If the reflection band of the chirped FBGs has a rectangular shape, $R(\lambda)$ is a constant. The detected power can be given by

$$P = \alpha TR \Delta\lambda_{\text{BW}} = \alpha TR \Delta\lambda_{\text{chirp}}, \quad (7)$$

where $\Delta\lambda_{\text{BW}}$ is the 3-dB bandwidth of the chirped FBG. If the reflectivity of the FBG keeps unchanged, there is a linear relationship between the detected power and the applied displacement.

Since temperature variation cannot change the reflection spectrum of the FBG and just cause the central wavelength shift of the FBG, the detected optical power is inherently insensitive to the temperature variation.

3. Experimental results and discussions

Fig. 2 shows the schematic configuration of the experimental setup. A C&L-bands broadband source (BBS) is used as the light source. After the reflected light passes through a circulator, it is divided into two paths via a 3 dB optical coupler, one is captured by an optical spectrum analyzer (OSA) and the other one is monitored by an optical powermeter. The applied displacement is controlled within the range of 0–3150 μm . Fig. 3 shows the reflection spectra of the chirped FBG under different displacements. With the increase of the displacement, the reflection spectrum

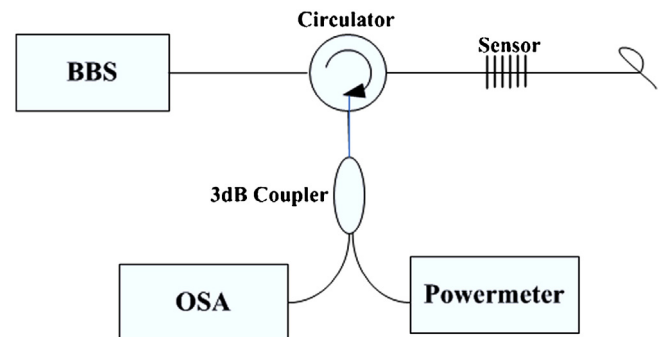


Fig. 2. Schematic configuration of the experimental setup.

Download English Version:

<https://daneshyari.com/en/article/736237>

Download Persian Version:

<https://daneshyari.com/article/736237>

[Daneshyari.com](https://daneshyari.com)